Microphase separation of rod-coil diblock copolymer in solution

Cite as: J. Chem. Phys. **130**, 094907 (2009); https://doi.org/10.1063/1.3078266
Submitted: 07 October 2008 . Accepted: 13 January 2009 . Published Online: 06 March 2009

Jiaping Lin, Shaoliang Lin, Liangshun Zhang, and Takuhei Nose

Microphase separation of rod-coil diblock copolymer in solution

Jiaping Lin,[1,a)] Shaoliang Lin,[1] Liangshun Zhang,[1] and Takuhei Nose[2]
[1]*Key Laboratory for Ultrafine Materials of Ministry of Education, School of Materials Science and Engineering, East China University of Science and Technology, Shanghai 20037, China*
[2]*Department of Nanochemistry, Tokyo Polytechnic University, Atsugi, Kanagawa 243-0297, Japan*

(Received 7 October 2008; accepted 13 January 2009; published online 6 March 2009)

Lattice theory of rigid rods is extended to describe the microphase separation behavior of a rod-coil diblock copolymer in solution. The free energy was formulated by inclusion of the energy terms arising from the core-corona interface between the rods and coils and the corona formed by the coils into the lattice model of rigid rods. The rod-coil diblock copolymer exhibits lyotropic mesophases with lamellar, cylindrical, and spherical structures when the copolymer concentration is above a critical value. The tendency of the rodlike blocks to form orientational order plays an important role in the formation of lyotropic phases. Influences of polymer-solvent interaction, surface free energy, and molecular architectures of the rod-coil diblock copolymer on the phase behaviors were studied, and phase diagrams were mapped accordingly. The theoretical results were compared with some existing experimental observations and a good agreement is shown. © *2009 American Institute of Physics*. [DOI: 10.1063/1.3078266]

I. INTRODUCTION

Theory of ordering transition of a polymer solution containing rigid rods was first proposed by Flory in terms of lattice model.[1,2] It was demonstrated that above a critical polymer concentration the polymer solution exhibits liquid crystalline ordered phase in which the rigid rods are arranged with their long axes parallel to each other. Later on this theory has been extended considerably to various liquid crystalline systems.[3–12] By the case of its applicability, the theory turns out to be highly useful in understanding the phase behaviors for manifold of systems. However, throughout the early theoretical considerations, the majority of polymers considered are homopolymers with rodlike conformation. If the rodlike polymer is covalently linked to a linear coiled polymer chain, the formed rod-coil block copolymer could share characteristics of both rodlike liquid crystalline polymer and diblock polymer. This rod-coil molecular architecture imparts microphase separation of the rod and coil blocks into ordered structures such as spherical, cylindrical, and lamellar microstructures. The supramolecular structures of the rod-coil polymers depend on a combination of organizing forces including the tendency of the rod blocks to form orientational order, the mutual repulsion of the dissimilar blocks, the interaction between polymer and solvent, and the packing constraints imposed by the connectivity of each block.[13–16]

The Flory lattice theory has already shed some light on the liquid crystalline phase behavior of the rod-coil copolymers. For example, Matheson and Flory extended the early lattice treatment to semirigid chains that contain inherent coil units at certain locations along the rigid chain.[8] It was found that when the coil segments are forced into the anisotropic phase, the degree of liquid crystalline order is decreased and the biphasic gap is narrowed. In their lattice treatments, the coil segment is regarded as a kind of diluent of the mesophase and has a degree of flexibility unaffected by the orientational order. Another case is a polymer with interconvertible rodlike and random-coil sequences. Polypeptide exhibiting a helix-coil transition is a prototypical example of this category. The lattice theoretical approach concerning this system was first carried out by Flory and Matheson[9] then by Lin and co-workers.[10–12,17] The free energy change for the coil-helix transition was incorporated into the lattice scheme by adopting an expression prescribed by Zimm and Bragg.[18] A marked broadening of the biphasic gap and its shift to higher polymer volume fractions were predicted as a result of the coil-to-helix transition when the coil segments enter the anisotropic phase. The equilibria of the helix-coil-type polymer are not unlike the case of alternating rigid-coil block copolymer. Formation of a liquid crystalline phase in such copolymers could be accompanied by the stiffening of the coil segments if the allowance is made for the conformation changes. However, in all these lattice treatments, the interaction between rodlike and coil blocks, which can give rise to microphase structures with local clustering of the rodlike blocks and randomly coil blocks, has not been considered. As stated in Ref. 8, the lattice model can be elaborated by inclusion of interfacial free energy terms in order to describe such systems.

Several theoretical attempts have already been made to deal with the microphase separation behavior of the rod-coil block copolymers in various conditions. For example, Semenov and Vasilenco initiated a study of melts of diblock copolymers consisting of a flexible tail connected to a rodlike block.[19] It was assumed that the tail and rodlike segments were incompatible, with the degree of incompatibility described via the Flory–Huggins parameter χ. At low enough χ values the rod-coil block copolymer exhibits a nematic

[a)]Author to whom correspondence should be addressed. Tel.: +86-21-64253370. FAX: +86-21-64253539. Electronic mail: jplinlab@online.sh.cn.

phase. The nematic phase changes to a smectic phase as the interaction parameter is increased. With further increasing χ the smectic phase is predicted to transform to a complete monolayer region where the coil chains are expelled completely from the rigid rod monolayers and followed by a bilayer lamellar phase. Halperin used scaling approach to predict the self-assembly structures of the rod-coil block copolymers in a selective solvent.[20] Formations of micellar and lamellar structures are found. The lamellas are predicted to exhibit a smectic A to smectic C transition driven by the competition between surface and coil chain deformation free energies. However, in his treatment the role of liquid crystal formation of rod blocks is not considered. Williams and Fredrickson presented a theoretical study of a melt of diblock copolymers consisting of a rigid and a flexible tail.[21] In addition to the formation of lamellar phases with various structures, they predicted a phase of hockey puck micelle, where the rods are packed axially into cylinders. Phase diagrams including the hockey puck and lamella phases were mapped. Studies on the microphase separation behaviors of the rod-coil block copolymer according to the self-consistent field theory and various simulation methods were also reported.[22–30] For example, Pryamitsyn and Ganesan employed the Flory–Huggins approach to model the enthalpic interactions between the rods and coils and the Maier–Saupe interaction to model the orientational interactions between rods.[24] In their two-dimensional calculations, nonlamellar structures, such as puck/broken lamellar, arrowhead, and zigzag phases, have been identified.

However, as far as we know, no studies based on the Flory lattice model have been carried out on the self-assembly of the rod-coil diblock copolymers driven by the liquid crystalline formation in solution. In the present work, the Flory lattice model is further generalized by including the free energies contributed from the core-corona interface and corona formation in order to describe the self-assembly of the rod-coil diblock copolymer in solution. Formations of lyotropic mesophases with spherical, lamellar, and cylindrical supramolecular structures were predicted and phase diagrams as functions of χ parameter, surface free energy γ, and molecular structure parameters were constructed.

II. THEORETICAL MODEL

The system under consideration contains an isodiametrical solvent and a diblock copolymer with an intrinsically flexible coil block A and a rodlike block B. The degrees of polymerization of the A and B blocks are N_A and N_B, respectively. The interaction between polymer chain and solvent is characterized by the Flory–Huggins parameter χ. Incompatibility of the rod and coil blocks manifests itself via a surface energy per unit (γ) at the interface between A and B aggregate areas. The solvent is not selective to either A or B blocks. In the dilute solution, the rod-coil block copolymer is well dissolved in the solvent to form an isotropic phase. When the polymer concentration is increased above a critical value, the rodlike blocks tend to form orientational order and lyotropic mesophases with lamellar, cylindrical, and spherical structures could be formed.[31] These structures are schemed in Fig. 1. The rodlike blocks are orientationally aligned to form the liquid crystal aggregate core and the coil blocks are expelled out of the core to form the corona. The liquid crystal aggregate core has height of L, which is assumed to be equal to N_B. The width and length of the core are X_{lamella} and X_{lamella}, X_{cylinder} and Y_{cylinder}, and X_{sphere} and X_{sphere} for lamella, cylinder, and sphere, respectively. The free energy F per chain for such aggregation structures is determined by the balance of the free energy of the core (F_{core}), the excess free energy of the core-corona interface $(F_{\text{interface}})$, and the free energy of corona (F_{corona}). It is written as

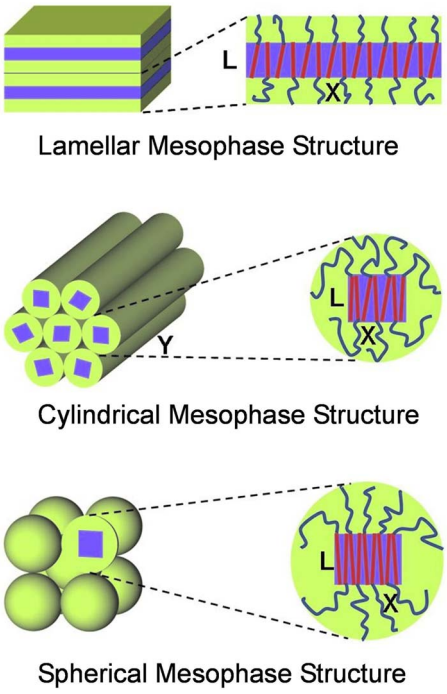

FIG. 1. (Color online) Schematic representation of the lyotropic mesophases with lamellar, cylindrical, and spherical structures. The gray (red) and dark gray (blue) lines denote the rod and coil blocks of the diblock copolymer, respectively.

$$F = F_{\text{core}} + F_{\text{interface}} + F_{\text{corona}}. \tag{1}$$

With respect to F_{core}, which is the driving force for the formation of lyotropic mesophase, we use the free energy expression for mixing of solvent and rigid rod prescribed by Flory.[1–3] In the present case, the rodlike blocks are placed within the core in the form of monolayer; therefore, the original free energy expression given by Flory should be modified. The detailed deduction of the modified expression is presented in the Appendix. Dividing the free energy [given by Eq. (A6)] by N_B/n_0, the free energy per chain is obtained as

$$F_{\text{core}} = N_B v_s \ln v_s + v_r \ln v_r - (N_B v_s + y v_r)\ln\left(v_s + \frac{y v_r}{N_B}\right) - v_r(\ln y^2 - y + 1) + \ln\frac{1+v_s}{4} + v_s \ln\frac{1+v_s}{v_s} + \chi N_B v_r v_s, \tag{2}$$

where v_s and v_r are the volume fractions of solvent and

rodlike block, n_0 is equal to $(n_s+n_pN_B)$, n_s and n_p are the numbers of solvent and rodlike block within the core. y is the disorientation index originally used in Flory's 1956 paper.[1]

According to Refs. 20 and 32, the excess free energy of the core-corona interface between liquid crystal core and coil chain corona (per chain) can be given by

$$F_{\text{interface}} = \gamma s v_r / n_p, \tag{3}$$

where s is the core-corona interface area for lamella, cylinder, and sphere aggregations, respectively.

Borisov and Zhulina prescribed a free energy expression (per chain) for the corona formed by coil chains of coil-coil diblock copolymer.[32] The aggregations are in the forms of lamella, cylinder, and sphere. Such an expression is written to be compatible with the present condition as follows:

$$F_{\text{corona}} = \frac{3^{8/3}}{2(4-i)}\left(\frac{\tau A_2}{iN_B}\right)^{1/3} R^{4/3} \times\left[\left(1+\frac{i+2}{3^{4/3}}\left(\frac{\tau A_2}{iN_B}\right)^{1/3}\frac{N_A}{R^{2/3}}\right)^{(4-i)/(i+2)} - 1\right], \tag{4}$$

where $i=1,2,3$ are for lamella, cylinder, and sphere, respectively, R is the radius of the aggregate core, which is equal to $N_B/2$, $(N_B^2+X_{\text{cylinder}}^2)^{1/2}/2$, and $(N_B^2+2X_{\text{sphere}}^2)^{1/2}/2$ for lamella, cylinder, and sphere, respectively,[32] A_2 is the effective second virial coefficient which is assumed to be $0.005/(0.5-\chi)$ in the present work, and τ is the polymer density in the core, which is equal to v_r in the present work.

As for a mixture consisting of a rod-coil diblock copolymer and a solvent in dilute isotropic condition, Matheson and Flory prescribed a free energy expression such as[8]

$$F_{\text{iso}} = n_s^i \ln v_s^i + n_p^i \ln\frac{v_p^i}{x} + (n_s^i + x n_p^i) \times\left[\left(1-\frac{1}{x}\right)v_p^i - v_c^i \ln Z_c + \chi v_s^i v_p^i\right] - n_p^i \ln \eta^2, \tag{5}$$

where n_s^i and n_p^i are the numbers of solvent and rod-coil polymers, v_s^i, v_p^i, and v_c^i are the volume fractions of solvent, copolymer, and coil, respectively, and x and η are the length of the copolymer and the rodlike block length which are equal to (N_A+N_B) and N_B in the present condition. In Flory and Matheson's treatment, Z_c is a statistical weight for the chain in coil state relative to the rodlike state, which was borrowed from the notion of the helix-coil theory for polypeptides.[18] In the present work, the energy difference between the coil and rodlike states is neglected for simplicity; thus Z_c becomes 1. Since the polymer chains are surrounded by the solvent molecules in the dilute solution, the interaction between the rod and coil is not considered. Incorporating these conditions into Eq. (5), the obtained expression of free energy per chain in dilute isotropic phase is

$$F_{\text{iso}} = (N_A+N_B)\left[v_s^i \ln v_s^i + \frac{1-v_s^i}{N_A+N_B}\ln\frac{1-v_s^i}{N_A+N_B} + \left(1-\frac{1}{N_A+N_B}\right)(1-v_s^i) - \frac{1-v_s^i}{N_A+N_B}\ln N_B^2 + \chi v_s^i(1-v_s^i)\right]. \tag{6}$$

III. NUMERICAL CALCULATIONS

For the system containing a nonselective solvent and a rod-coil block copolymer, isotropic phase forms at lower polymer concentrations. When the polymer concentration is increased above a critical value, the rod-coil block copolymers form lyotropic mesophase with lamellar, cylindrical, and spherical structures. The orientational order formation of the rodlike block is the main driving force for incipience of the anisotropic phase structures. The free energy expressions (per chain) for the above system which can form lyotropic phases with spherical, cylindrical, and lamellar structures are given by Eqs. (1)–(4) as a function of the corresponding core size. Minimization of F with respect to core sizes [X_{lamella}, (X_{cylinder}, Y_{cylinder}), and X_{sphere}] gives equilibrium core size at given conditions. The corresponding equilibrium corona size is dependent on the core size and their relation is given by[32]

$$D(R) = R\left[1+\frac{i+2}{3^{4/3}}\left(\frac{\tau A_2}{iN_B}\right)^{1/3}\frac{N_A}{R^{2/3}}\right]^{3/(i+2)}, \tag{7}$$

where D is the radius of the corona. Using the equation together with the condition

$$\frac{N_A+N_B}{v_p} = \frac{N_A}{v_c} + \frac{N_B}{v_r}, \tag{8}$$

where v_c is the volume fraction of coils in the corona, the volume fraction of rodlike block, v_r, can be converted to the overall volume fraction of the diblock copolymer, v_p, in the system. The phase diagrams as a function of v_p thus can be obtained. In addition, Eq. (6) gives the free energy of the isotropic phase. The transitions between various phases including isotropic phase and phases of spherical, cylindrical, and lamellar aggregations occur when the corresponding equilibrium free energies are equal. This determines the binodal line between the neighboring morphologies.

Figure 2 shows a typical phase diagram where the χ parameter is plotted against volume fraction of the block copolymer, v_p. The diagram contains regions corresponding to the isotropic phase (I), spherical (S), cylindrical (C), and lamellar (L) lyotropic phases. The isotropic phase where the block copolymer is well dissolved in the solvent is exhibited when the polymer concentration v_p is lower. Increasing v_p to a critical value, rodlike blocks are orientationally aligned to form liquid crystal aggregate core and the coil blocks are expelled out of the core to form the corona due to the incompatibility between the rods and coils. Further increase in v_p leads to successive transitions from lamella to cylinder then to sphere. The phase boundaries of the isotropy-lamella, lamella-cylinder, and cylinder-sphere shift to higher polymer concentrations when the χ value decreases.

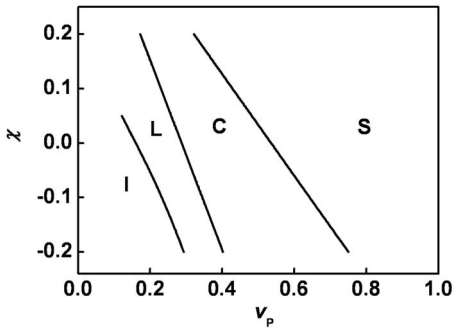

FIG. 2. Phase diagram of rod-coil diblock copolymer in solution. The ordinate is the polymer-solvent interaction parameter χ, while the abscissa is the volume fraction of the block copolymer, v_p. Invariant parameters used in the calculations are $N_A=200$, $N_B=200$, and $\gamma=0.40$. I: isotropic phase, L: lamellar aggregation region, C: cylindrical aggregation region, S: spherical aggregation region.

The role of the surface free energy per unit, γ, which is associated with the incompatibility between N_A and N_B blocks, is illustrated in Fig. 3. The isotropic phase is stable at low concentrations of the block copolymer, v_p. The phase boundary between the isotropic and lamellar phase is nearly vertical, indicating that the change in γ value has a weak effect on the concentration for the anisotropic phase formation. However, with respect to the phase boundaries of the lamella-cylinder and cylinder-sphere, they shift toward higher polymer concentrations as γ is increased. This implies that the interaction between N_A and N_B blocks as manifested by γ plays an important role in determining the aggregation morphologies. At a certain value of v_p, for example, $v_p=0.3$, increase in miscibility between coils and rods (γ becomes greater) leads to sphere→cylinder→lamella transitions. In the phase diagram there also exists a triple point where isotropic, lamellar, and cylindrical phases meet. Above this point the isotropic phase transforms to lamellar and cylindrical phases successively as v_p is increased, while below this point the isotropic phase transforms directly to cylindrical phase then spherical phase with increasing the v_p value. It should be noted that the stability regions of various microstructures are determined by the balance of the free energies of core, corona, and core-corona interface, which

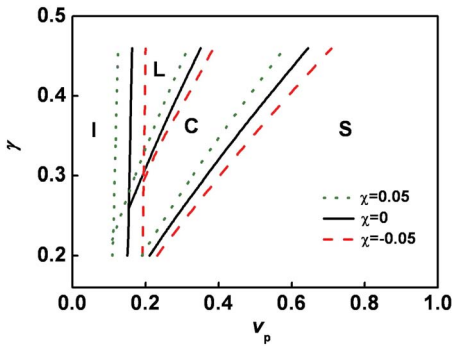

FIG. 3. (Color online) Phase diagram of rod-coil diblock copolymer in solution calculated for $\chi=-0.05$, 0, and 0.05. The ordinate is surface energy per unit γ, while the abscissa is the volume fraction of the block copolymer, v_p. Invariant parameters used in the calculations are $N_A=200$ and $N_B=200$. I: isotropic phase, L: lamellar aggregation region, C: cylindrical aggregation region, S: spherical aggregation region.

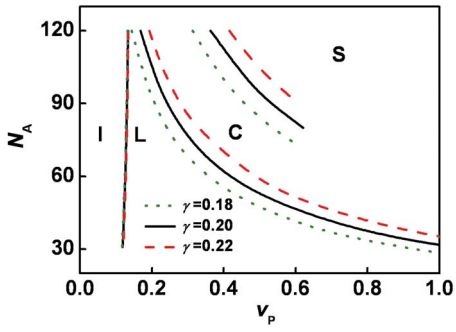

FIG. 4. (Color online) Coil block length N_A plotted against v_p at $\gamma=0.18$, 0.20, and 0.22. Invariant parameters used in the calculations are $N_B=300$ and $\chi=0$.

depends on various parameters, such as block lengths and polymer-solvent interaction parameter χ. The phase regions can be tuned by the variation of these parameters. For example, at high enough value of γ, only stable lamellar phase is expected to exist. Figure 3 also shows the influence of χ on the stability region. The χ values of -0.05, 0, and 0.05 were adopted in the calculations. As can be seen, the phase regions including isotropy, sphere, cylinder, and lamella shift to lower polymer concentrations when the value of χ is increased.

Figure 4 shows the effect of the coil block length on the phase equilibria of the diblock copolymer at a given length of rodlike block. The lamellar phase is dominant when N_A is small. When the coil block length is increased, the lamellar phase transforms to cylindrical phase then to spherical phase. It is also noted that change in coil length has less pronounced effect on polymer concentration for the isotropy-anisotropy transition. This can be attributed to the fact that the liquid crystal formation is governed by the aggregation of the rodlike blocks. Increasing N_A while keeping the N_B unchanged should have a weak influence on the isotropy-anisotropy phase boundary. In Fig. 4, phase diagrams are shown for $\gamma=0.18$, 0.20, and 0.22. With increasing γ value from 0.18 to 0.22, the lamella-cylinder and cylinder-sphere phase boundaries shift upwards. However, less marked change is shown for the isotropy-anisotropy transition.

Effect of variation of N_B at a given N_A is illustrated in Fig. 5. As can be seen, the polymer concentration for the formation of anisotropic lamellar phase decreases as the rodlike block length is increased. This is in agreement with the

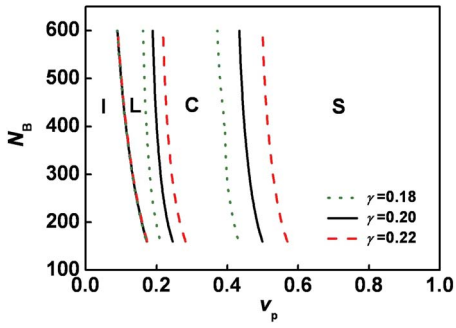

FIG. 5. (Color online) Rodlike block length N_B plotted against v_p at $\gamma=0.18$, 0.20, and 0.22. Invariant parameters used in the calculations are $N_A=100$ and $\chi=0$.

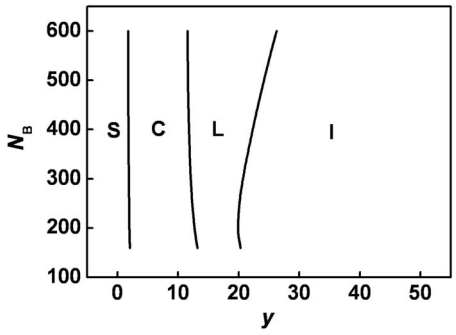

FIG. 6. Rodlike block length N_B plotted against disorientation index y. Invariant parameters used in the calculations are $N_A=100$, $\chi=0$, and $\gamma=0.20$.

prediction of the lattice theory of rigid rods, i.e., the longer the rigid rod, the lower the incipient polymer concentration for the anisotropic formation.[1–3] As for the lamella-cylinder and cylinder-sphere phase boundaries, both shift toward lower polymer concentrations with increasing N_B. The influence of the change in γ on the phase diagram is also shown in Fig. 5. When the γ value increases from 0.18 to 0.22, the lamella-cylinder and cylinder-sphere phase boundaries shift to higher polymer concentrations. However, the shift of the isotropy-anisotropy phase boundary is negligible.

Since the preference of the rodlike blocks to form orientational order plays an important role in forming lyotropic mesophases, we further examined the relationship between the orientational order of rods and the mesophase behavior. Dependence of orientational order of the rodlike blocks within the core on the phase behavior is shown in Fig. 6 where N_B is plotted against disorientation index y. When the orientational order of the rodlike blocks is higher, corresponding to smaller y values, the spherical aggregation is observed. As the rodlike blocks become less orderly aligned (y turns greater), the spherical phase transforms to cylindrical phase then lamellar phase. Finally, the isotropic phase appears at higher disorder of the rodlike blocks. From Fig. 6 the N_B dependence of the order-disorder transition can also be seen. The isotropy-lamella phase boundary shifts to higher y values when N_B is increased. This is expected since the driving force to form anisotropy becomes stronger when the N_B value is greater.

IV. DISCUSSION

Self-assembly of the block copolymers through microphase separation has great potentials for creating supramolecular structures with well-defined shapes and functions.[31,33,34] So far much attention has been paid to the coil-coil diblock copolymers which are found to exhibit a wide range of microphase separated structures. Such phase behavior is understood to be mainly due to the mutual repulsion of the dissimilar blocks and the packing constraints imposed by the connectivity of each blocks. In comparison with the extensive studies on the coil-coil diblock copolymers, the phase behaviors of the rod-coil diblock copolymers, especially in solution, are not well understood. From the present work, we learned that the isotropic to anisotropic phase transition of the rod-coil diblock is governed by the tendency of the rodlike blocks to form orientational order (lyotropic mesophases form when v_p is above a critical value). The liquid crystalline formation is the driving force for incipience of the anisotropic phase structures. On the other hand, the microphase separated structures such as lamella, cylinder, and sphere are mainly determined by the mutual repulsion of the dissimilar rod and coil blocks. The incompatibility of the rod and coil blocks manifesting itself via the surface energy at the interface between A block and B block aggregate areas plays an important role in determining the areas of the stability region of lamellar, cylindrical, and spherical aggregations, as can be seen in Figs. 4 and 5.

Some experimental and simulation evidences are available in the literatures for testing of our theory. Douy *et al.* examined the phase structures of a rod-coil diblock copolymer consisting of a polypeptide block in helix conformation as the rodlike block.[35] Lamellar mesophase was observed in aqueous solution by x-ray diffraction. Each sheet of the lamellar structure contains two layers: one formed by the rodlike polypeptide block packed with their long axes aligned and the other formed by the flexible chains arranged in a random fashion. The helix rods are found to be tilted on the plane of the lamellas and assembled in a hexagonal array. This experimental observation is generally consistent with the present theoretical work, i.e., the rod-coil copolymers can self-associate into lamellar structure in solution above a critical polymer concentration, and the rod blocks are arranged with their long axes parallel to each other within the layer of lamella. Our theoretical work is also supported by some simulation results. For example, Alsunaidi *et al.* studied the liquid crystalline ordering in rod-coil diblock copolymers using dissipative particle dynamics simulations.[26] Lamella mesophase was found for the rod-coil diblock copolymers. The rods align to form the ordered layer, while the coils randomly pack to form the disordered layer. Although the simulations were performed in melt state, the obtained results can correspond to the situations at higher v_p in present work. The DPD simulations show a qualitative match with the present theory.

Lee *et al.* studied the self-organization of the rod-coil molecules consisting of a mesogenic rod and a propylene oxide with various lengths.[15] The rod-coil molecules with 7 and 8 propylene oxide units exhibit layered smectic phase, while the rod-coil molecules with 10–15 repeating units exhibit a discontinuous cubic mesophase. Further increasing the length of the coil induces a hexagonal columnar mesophase. Such experiments carried out in the melt state are not unlike the case when the value of v_p is greater in the present work. The experimental observed smectic and hexagonal columnar mesophases can correspond to the lamellar and cylindrical phases in our theory. As can be seen from Fig. 4, at higher value of v_p, transition from lamella to cylinder phase takes place when the coil length increases. The general tendency of the phase transition predicted by the theory is consistent with the experimental observations, except for the corresponding discontinuous cubic mesophase which does not exist in the theory.

Finally, we wish to emphasize that the Flory lattice mode, despite its artificiality, has proved successful in the

treatments of the phase behaviors of the rodlike polymers. The versatility of this theory has permitted its extensions to various systems.[3–12] In the present work, we extended the lattice model of rigid rods to the rod-coil diblock copolymers and give another example of the versatility of the lattice theory. After incorporating the free energy terms contributed from the core-corona interface and corona formed by the coil chains into the lattice scheme, the theory provides a reasonable insight for the phase behaviors of the rod-coil diblock copolymer. It should be emphasized that orientation-dependent interactions between the rigid rods could promote the liquid crystallinity. However, the dominant molecular characteristic responsible for the liquid crystals appears invariably to be asymmetry of molecules, especially in solution where the molecules are surrounded by solvents.[2] For simplicity, we only consider the asymmetry of molecules in the present work. The importance of the contribution of the orientation-dependent interactions will be studied in our further work. Moreover, in the present work, only three basic microphase structures, i.e., sphere, cylinder, and lamella, are considered for simplicity. The rod-coil diblock copolymer may have some more complicated microphase structures, such as bilayer lamella structure and lamella with the rod tilted. The present theoretical model is ready to be elaborated by inclusion of the corresponding free energy contributions in order to describe these self-assembled microphase structures.

V. CONCLUSION

In summary, we extended the lattice model of rigid rods to the rod-coil diblock copolymers. The free energy was formulated by inclusion of the energy terms arising from the core-corona interface between the rods and coils and the corona formed by the coils into the lattice model of rigid rods. The rod-coil diblock copolymer exhibits lyotropic mesophases with lamellar, cylindrical, and spherical microstructures when the copolymer concentration (v_p) is above a critical value. The isotropic to anisotropic phase transition of the rod-coil diblock is governed by the tendency of the rod blocks to form orientational order structure, while the microphase separated structures such as lamella, cylinder, and sphere are mainly determined by the mutual repulsion of the dissimilar rod and coil blocks. Influences of polymer-solvent interaction, surface free energy, and molecular architectures of the rod-coil diblock copolymer on the phase behaviors were studied, and phase diagrams were mapped accordingly.

ACKNOWLEDGMENTS

This work was supported by the National Natural Science Foundation of China (Grant No. 50673026) and Chenguang Project of Shanghai (Grant No. 2007CG38). The authors wish to thank Professor Akihiro Abe of Tokyo Polytechnic University for his most helpful advice and stimulating discussions.

APPENDIX: FREE ENERGY FOR RODLIKE BLOCKS PLACED WITHIN THE AGGREGATION CORE IN MONOLAYER FORM

Based on the Flory lattice model, the rodlike block with axis ratio N_B inclined to the orientation axis is divided into y submolecules, each containing N_B/y segments and requiring therefore N_B/y vacant lattice cells. The parameter y originally used in Flory's 1956 paper serves as a measure of the orientation of the rods with respect to the liquid crystal core. We propose that $j-1$ rodlike blocks have been assigned locations in the volume with the total number n_0 of lattice sites and the first segments of rodlike blocks are restrained in the cuboid surface as shown in Fig. 1. Following the approximation employed by Flory, the number of sites available to the first segments of rod j, consisting of y_j submolecules, is $2(n_0/N_B)-(j-1)$, where $2(n_0/N_B)$ is the number of lattice sites in the cuboid surface.

The probability that each succeeding site is vacant in the row is given by the ratio of vacant sites to the sum of vacant sites and submolecules.[1] Hence, the probability that the N_B/y_j-1 sites required for the remaining segments of the first submolecules are vacant is

$$\left[\frac{n_0-N_B(j-1)}{n_0-N_B(j-1)+\sum_{i=1}^{j-1}y_i}\right]^{N_B/y_j-1}. \tag{A1}$$

The probability of vacancy in the lattice site for the first segment of the second submolecule is $(n_0-N_B(j-1))/n_0$. A factor like that given above is required for the remaining segments of the second submolecule, etc. Combining these factors, we obtain the number v_j of situations available to an additional rodlike block j by

$$v_j=\left[2\frac{n_0}{N_B}-(j-1)\right]\left[\frac{n_0-N_B(j-1)}{n_0-N_B(j-1)+\sum_{i=1}^{j-1}y_i}\right]^{N_B-y_j}\times\left[\frac{n_0-N_B(j-1)}{n_0}\right]^{y_j-1}. \tag{A2}$$

Introduction of y for the average $(j-1)^{-1}\Sigma_{i=1}^{j-1}y_i$ and combination of factors yields

$$v_j=\frac{2\frac{n_0}{N_B}-(j-1)}{n_0-N_B(j-1)}\frac{[n_0-N_B(j-1)]^{N_B}}{[n_0-(N_B-y_j)(j-1)]^{(N_B-y_j)}n_0^{(y_j-1)}}. \tag{A3}$$

Supposing total number n_p of rodlike blocks to be assigned in the cuboid, then combinatory factor Z_{comb} can be written by introduction of Stirling's approximations as

$$Z_{\text{comb}} = \frac{1}{n_p!}\prod_{j=1}^{n_p} v_j = \frac{[n_s + yn_p]!}{n_s!\, n_p!\, (n_0)^{n_p(y-1)}} \frac{\left[2\frac{n_0}{N_B}\right]! \left[\frac{n_0}{N_B} - n_p\right]!}{N_B^{n_p}\left[2\frac{n_0}{N_B} - n_p\right]! \left[\frac{n_0}{N_B}\right]!}, \tag{A4}$$

where $n_s = n_0 - n_p N_B$ are the remaining vacant sites, which is occupied by solvents.

The configuration partition function Z for mixture of rodlike blocks and solvents is the product of combinatory and orientational factors Z_{comb} and Z_{orient}, respectively, where Z_{orient} can be written by $(y/N_B)^{2n_p}$.[1] Then,

$$\begin{aligned} -\ln Z &= -\ln(Z_{\text{comb}} Z_{\text{orient}}) = n_s \ln v_s + n_p \ln v_r \\ &\quad - (n_s + yn_p)\ln\frac{n_s + yn_p}{n_0} - n_p(\ln y^2 - y + 1) \\ &\quad + \left(n_p + \frac{n_s}{N_B}\right)\ln\frac{1+v_s}{4} + \frac{n_s}{N_B}\ln\frac{1+v_s}{v_s}, \end{aligned} \tag{A5}$$

where $v_s = n_s/n_0$ and $v_r = n_p N_B/n_0$ are the volume fractions of solvent and rodlike blocks, respectively.

Moreover, the heat of mixing can be given by $\chi N_B n_p v_s$,[1,2] where χ is the Flory–Huggins interaction between rodlike block and solvent. Thus, the free energy of mixing for rodlike blocks placed with aggregation core in monolayer form is obtained as

$$\begin{aligned} -\ln Z &= n_s \ln v_s + n_p \ln n_p - (n_s + yn_p)\ln\frac{n_s + yn_p}{n_0} \\ &\quad - n_p(\ln y^2 - y + 1) + \left(n_p + \frac{n_s}{N_B}\right)\ln\left(\frac{1+v_s}{4}\right) \\ &\quad + \frac{n_s}{N_B}\ln\left(\frac{1+v_s}{v_s}\right) + \chi N_B n_p v_s. \end{aligned} \tag{A6}$$

[1] P. J. Flory, Proc. R. Soc. London, Ser. A **234**, 73 (1956).
[2] P. J. Flory, Adv. Polym. Sci. **59**, 1 (1984).
[3] A. Abe and M. Ballauff, *Liquid Crystallinity in Polymers* (VCH, New York, 1991), pp. 131–167.
[4] A. Abe and P. J. Flory, Macromolecules **11**, 1122 (1978).
[5] R. S. Frost and P. J. Flory, Macromolecules **11**, 1134 (1978).
[6] P. J. Flory, Macromolecules **11**, 1138 (1978).
[7] P. J. Flory, Macromolecules **11**, 1141 (1978).
[8] R. R. Matheson and P. J. Flory, Macromolecules **14**, 954 (1981).
[9] P. J. Flory and R. R. Matheson, J. Phys. Chem. **88**, 6606 (1984).
[10] J. Lin, A. Abe, H. Furuya, and S. Okamoto, Macromolecules **29**, 2584 (1996).
[11] J. Lin, S. Lin, P. Liu, T. Hiejima, H. Furuya, and A. Abe, Macromolecules **36**, 6267 (2003).
[12] J. Lin, S. Lin, T. Chen, and X. Tian, Macromolecules **37**, 5461 (2004).
[13] M. Lee, B. K. Cho, and W. C. Zin, Chem. Rev. (Washington, D.C.) **101**, 3869 (2001).
[14] M. Lee, N. K. Oh, H. K. Lee, and W. C. Zin, Macromolecules **29**, 5567 (1996).
[15] M. Lee, B. K. Cho, H. Kim, J. Y. Yoon, and W. C. Zin, J. Am. Chem. Soc. **120**, 9168 (1998).
[16] S. Lecommandoux, H.-A. Klok, and H. Schlaad, *Block Copolymer in Nanoscience* (Wiley-VCH Press, Weinheim, 2006), p. 117.
[17] T. Chen, S. Lin, J. Lin, and L. Zhang, Polymer **48**, 2056 (2007).
[18] B. H. Zimm and J. K. Bragg, J. Chem. Phys. **31**, 526 (1959).
[19] A. N. Semenov and S. V. Vasilenco, Sov. Phys. JETP **63**, 70 (1986).
[20] A. Halperin, Macromolecules **23**, 2724 (1990).
[21] D. R. M. Williams and G. H. Fredrickson, Macromolecules **25**, 3561 (1992).
[22] R. R. Netz and M. Schick, Phys. Rev. Lett. **77**, 302 (1996).
[23] M. Muller and M. Schick, Macromolecules **29**, 8900 (1996).
[24] V. Pryamitsyn and V. Ganesan, J. Chem. Phys. **120**, 5824 (2004).
[25] J. Chen, C. Zhang, Z. Sun, Y. Zheng, and L. An, J. Chem. Phys. **124**, 104907 (2006).
[26] A. Alsunaidi, W. K. den Otter, and J. H. R. Clarke, Philos. Trans. R. Soc. London, Ser. A **362**, 1773 (2004).
[27] N. Yamazaki, M. Motoyama, M. Nonomura, and T. Ohta, J. Chem. Phys. **120**, 3949 (2004).
[28] L. Cheng and D. Cao, J. Chem. Phys. **128**, 074902 (2008).
[29] M. A. Horsch, Z. Zhang, and S. C. Glotzer, Phys. Rev. Lett. **95**, 056105 (2005).
[30] S. Lin, N. Numasawa, T. Nose, and J. Lin, Macromolecules **40**, 1684 (2007).
[31] I. W. Hamley, *Block Copolymers in Solution: Fundamentals and Applications* (Wiley, Chichester, 2005).
[32] O. V. Borisov and E. B. Zhulina, Macromolecules **36**, 10029 (2003).
[33] F. Forster and T. Plantenberg, Angew. Chem., Int. Ed. **41**, 688 (2002).
[34] F. Forster and M. Antonietti, Adv. Mater. (Weinheim, Ger.) **10**, 195 (1998).
[35] A. Douy and B. Gallot, Polymer **28**, 147 (1987).